Acta Crystallographica Section A
Foundations of Crystallography
ISSN 0108-7673
Editor: **D. Schwarzenbach**

Data scaling and temperature calibration in time-resolved photocrystallographic experiments

Mette S. Schmøkel, Radosław Kamiński, Jason B. Benedict and Philip Coppens

Acta Cryst. (2010). A**66**, 632–636

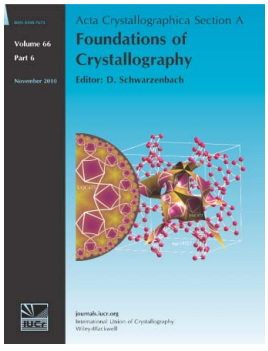

Acta Crystallographica Section A
Foundations of Crystallography
ISSN 0108-7673

Received 20 May 2010
Accepted 23 July 2010

Data scaling and temperature calibration in time-resolved photocrystallographic experiments

Mette S. Schmøkel,[a,b] Radosław Kamiński,[a,c] Jason B. Benedict[a] and Philip Coppens[a]*

[a]Department of Chemistry, University at Buffalo, The State University of New York, Buffalo, NY 14260-3000, USA, [b]Department of Chemistry, Aarhus University, Langelandsgade 140, DK-8000 Aarhus C, Denmark, and [c]Department of Chemistry, University of Warsaw, Pasteura 1, 02-093 Warszawa, Poland. Correspondence e-mail: coppens@buffalo.edu

Experiments in which structural changes in crystals are induced by pulsed-laser exposure involve an increase in sample temperature due to the dissipation of the deposited excess energy. The heat increase is especially pronounced when a large number of pulses is needed, as in pseudo-steady-state experiments conducted at conventional sources, but not negligible in synchrotron studies in which very short laser exposures may be adequate. The relative scaling of the light-ON and light-OFF data and the correction for temperature differences between the two sets are discussed.

1. Introduction

Time-resolved studies of light-induced short-lived species in molecular crystals have recently attracted considerable attention and have been reported in recent special issues of *Acta Crystallographica Section A* (Collet, 2010) and the *Zeitschrift für Kristallographie* (Woike & Schaniel, 2008). The understanding of the processes that occur when crystals are exposed to laser light is relevant to the design of molecular electronics and non-linear optical devices. Such processes can now be studied at the atomic level using time-resolved photocrystallographic techniques. Both monochromatic and polychromatic radiation have been used in such studies, the latter exclusively at synchrotron sources. The former is most useful when lifetimes are of the order of μs or more, whereas polychromatic radiation is currently essential when time resolution in the fs–ps range is desired. Monochromatic experiments can be performed at both synchrotron and home-based X-ray sources, especially with the brighter commercial X-ray sources which have recently become available. Interpretation of the data requires that basic problems related to light-induced temperature changes and the relative scaling of light-ON and light-OFF data be addressed, as discussed below. Temperature scaling is of particular importance for experiments at conventional sources in which many laser pulses are required to collect meaningful X-ray data. Temperature effects are much smaller in synchrotron pump–probe experiments, which can be performed with a very limited number of laser pulses. In ultrafast sub-nanosecond experiments the data can be recorded before the temperature increase occurs; in all other cases it has to be taken into account in the analysis of the data.

2. The response ratio refinement formalism

Two descriptors of light-induced changes in photocrystallographic experiments are the intensity ratio R and the fractional change or response ratio η. They are defined as

$$R_{\rm ON/OFF}(\mathbf{h}) = \frac{I_{\rm ON}(\mathbf{h})}{I_{\rm OFF}(\mathbf{h})} = \frac{\left|F_{\rm ON}(\mathbf{h})\right|^2}{\left|F_{\rm OFF}(\mathbf{h})\right|^2}, \quad (1)$$

$$\eta_{\rm ON/OFF}(\mathbf{h}) = \frac{I_{\rm ON}(\mathbf{h}) - I_{\rm OFF}(\mathbf{h})}{I_{\rm OFF}(\mathbf{h})} = R_{\rm ON/OFF}(\mathbf{h}) - 1, \quad (2)$$

where $I_i(\mathbf{h})$ is the intensity of the reflection with reciprocal vector $\mathbf{h}$ for either the light-ON or light-OFF experiment and $F_i(\mathbf{h})$ is the corresponding structure factor (Coppens *et al.*, 2010). As a result of the presence of laser-induced species and temperature increases, R values are mostly smaller than 1.0, and thus the response ratios tend to be negative.

The most sensitive refinement of laser-induced changes is based on the response ratios (Ozawa *et al.*, 1998; Vorontsov & Coppens, 2005; Vorontsov *et al.*, 2010). In such a least-squares refinement the error function minimized is defined as

$$S_\eta = \sum_{\mathbf{h}} w(\mathbf{h})\left|\eta_{\rm o}(\mathbf{h}) - \eta_{\rm c}(\mathbf{h})\right|^2, \quad (3)$$

where $\eta_{\rm o}$ and $\eta_{\rm c}$ are the observed and calculated response ratios, respectively, and w is the appropriate weight. If desired, parameters of both the ground and the excited states can be refined, and if unit-cell changes are significant, different unit cells can be used for the two structures. The temperature increases on illumination can be taken into account through

inclusion of an overall temperature scale parameter k_B applied to the light-ON data:

$$U_{ij,\mathrm{ON}} = k_B U_{ij,\mathrm{OFF}}. \quad (4)$$

It multiplies all U_{ij} values and thus assumes that the increase is proportional to the lower-temperature values.

For the calculation of photo-difference maps and reliable response ratios it is crucial that both data sets are on the same scale. This is not a problem when the measurement of single light-ON frames is alternated by that of the corresponding light-OFF frames, as is typically the case in synchrotron pump–probe experiments in which single-pulse or stroboscopic techniques are used. In that case the two data sets will be on the same scale. However, when the experiments are performed at home sources with high-repetition-rate or steady-state lasers, the two data sets are collected consecutively and are typically not on identical scales. Such scaling can be achieved by use of Wilson-type plots, which are capable of normalizing data sets affected by thermal processes, the timescales of which are governed by equilibration through acoustic modes in crystals. Their propagation times are volume dependent. The Wilson plots are described in the following section.

3. Photo-Wilson plots

3.1. Estimate of temperature difference based on statistical analysis

The well known Wilson plot is commonly used to obtain initial estimates of the scale factor, k_S, of a data set and the overall isotropic temperature factors. It is based on intensity statistics which show that in each $\sin\theta/\lambda$ range the average squared structure factor equals $\sum_{i=1}^{M} f_i^2$ for that range, or

$$\left|F_\mathrm{o}(\mathbf{h})\right|^2 = k_S^2\left(\sum_{i=1}^{M} f_i^2\right)\exp\left[-2Bs^2(\mathbf{h})\right], \quad (5)$$

where $F_\mathrm{o}(\mathbf{h})$ is the observed structure factor, M is the number of atoms, f_i is the scattering factor of the ith atom, B is the isotropic temperature factor and $s(\mathbf{h}) = \sin\theta/\lambda$.

A modified Wilson plot was applied to estimate the laser-induced temperature increase in the time-resolved pump–probe study of the binuclear platinum ion $Pt_2(H_2P_2O_5)^{4-}$ (Kim *et al.*, 2002) and has recently been used in a study of the temperature fluctuation as a function of time (Cailleau *et al.*, 2010). In such a photo-Wilson plot the ratio of the light-ON and light-OFF intensities is plotted to estimate the *difference* in temperature in the crystal during the laser-ON and laser-OFF measurements. From equation (5) it follows that

$$\ln\left[R_{\mathrm{ON/OFF}}(\mathbf{h})\right] = -2\Delta B s^2(\mathbf{h}) + b, \quad (6)$$

where $\Delta B = B_\mathrm{ON} - B_\mathrm{OFF}$. ΔB is related to the temperature scale parameter k_B defined in equation (4) through the expression

$$k_B = 1 + \frac{\Delta B}{8\pi^2\left\langle U_{\mathrm{eq,OFF}}\right\rangle} \quad (7)$$

where $\left\langle U_{\mathrm{eq,OFF}}\right\rangle$ is an average over the atoms in the light-OFF structure.

Model calculations show that ΔB obtained in this way contains a moderate contribution from the photo-induced disorder and thus affects $\sum f_i^2$. This tends to introduce a $\sin\theta/\lambda$-dependent decrease in the intensities (Vorontsov & Coppens, 2005).

3.2. The relative scale of the light-ON and light-OFF data sets

The number of electrons in the unit cell is the same in the light-OFF and light-ON crystal structures, *i.e.* $F_\mathrm{ON}(000) = F_\mathrm{OFF}(000)$ so that $R_\mathrm{ON/OFF}(000) = 1.0$ when both data sets are on the same scale. Thus the constant b in equation (6) may be expected to equal 0.0. This is the case in the synchrotron pump–probe experiment in which light-ON- and light-OFF-frame measurements rapidly alternate (Kim *et al.*, 2002). However, in experiments at conventional sources the light-OFF and light-ON data sets are measured consecutively, sometimes on different crystals with different exposure times, and will therefore in general be on a different scale. Separate least-squares refinement of the two data sets based on models for the ground-state and partially-excited-state structures is not feasible as the correct model for the excited state and the level of population of the excited molecules are still to be determined. Use of only the ground-state positional and thermal parameters for estimation of the scale of the light-ON data will lead to biased scaling.

However, the constant b in equation (6) is related to the ratio of the scale factors in the ON and OFF data sets by

$$b = \ln\left(k_{S,\mathrm{ON}}^2/k_{S,\mathrm{OFF}}^2\right). \quad (8)$$

Thus light-ON data can be brought to the same scale as the light-OFF data by multiplication by the value of $\exp(-b)$. This allows photo-difference maps and response ratios to be calculated. The potential of this procedure is considerable as it makes it possible to collect the light-OFF and light-ON data sets with different exposure times and on crystals of different size. The latter is of particular importance as, due to the limited penetration of the laser beam in absorbing solids, very small crystals must be used for the collection of the light-ON data.

4. Practical application of the formalisms

To test the applicability of the expressions, the above approach has been applied to data of the [bis(4-chlorothiophenyl)-1,10-phenanthroline]zinc(II) complex. Single-crystal light-OFF and light-ON data sets were collected using Mo $K\alpha$ monochromatic radiation from a Rigaku RU-200BEH rotating-anode X-ray generator at temperatures of 30 and 90 K. An average laser power of ~5.9 μJ and a repetition rate of 20 kHz were used. The data sets were separately integrated with the program *SAINT* (Bruker, 2007), corrected for Lorentz and polarization effects, and then scaled with *SORTAV*. The program *SORTAV* (Blessing, 1995, 1997) was also used for absorption corrections and merging of the data.

4.1. Scaling of the data sets

In order to calculate the photo-Wilson plots, the $\sin\theta/\lambda$ values of the reflections were calculated with the light-OFF unit cell at 30 K (Table 1). Using the light-ON unit cell leads to essentially the same plots.

The photo-Wilson plot presented in Fig. 1(*a*) is calculated before the relative scaling of the two data sets. The resulting *b* parameter equals −0.144 (5). Estimating the relative scaling of the two sets by refinement of the scale factor in *SHELXL* (Sheldrick, 2008) results in the photo-Wilson plot presented in Fig. 1(*b*). For both data sets the same structural model, containing only the ground-state structure, was used. This implies that the k_S parameter for the light-ON data is biased by the incorrectness of the structural model. The value of b = 0.447 (7) is, as expected, different from the value obtained from the raw data. After correcting the light-ON data for the improper scaling based on the value of *b* the fitted line in the photo-Wilson plot passes through the origin, as expected (Fig. 1*c*), indicating that both sets are on the same scale as needed for the response ratio refinement. The ΔB parameter is not affected by this scaling.

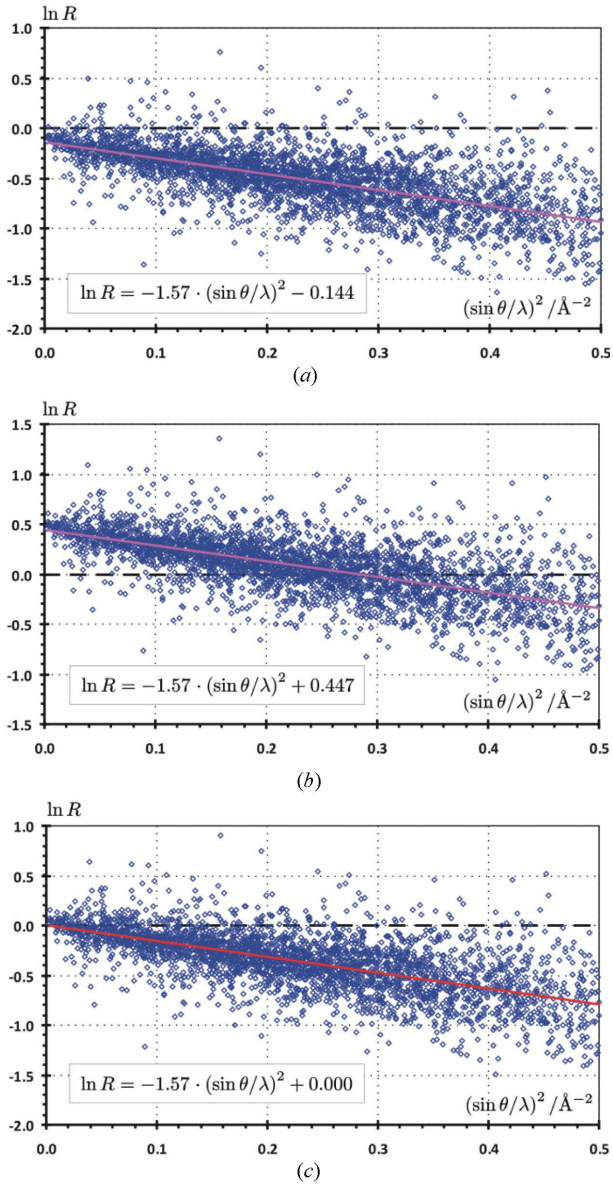

Figure 1
The photo-Wilson plots for 30 K light-OFF and light-ON data obtained by comparison of (*a*) raw unscaled intensities, (*b*) intensities which are brought on the absolute scale by scale-factor refinement using the ground-state structural model and (*c*) data from (*b*) corrected for the error in scaling of the light-ON data. In all cases only reflections with $I > 3\sigma(I)$ were included.

Table 1
Unit-cell parameters for light-OFF and light-ON structures at two different temperatures.

Data set	Light-OFF (30 K)	Light-ON (30 K)	Light-OFF (90 K)
a (Å)	10.9437 (10)	10.9679 (12)	10.9663 (9)
b (Å)	11.7421 (11)	11.7676 (13)	11.7900 (9)
c (Å)	17.1816 (16)	17.1977 (19)	17.1743 (13)
α (°)	90	90	90
β (°)	91.7063 (29)	91.5871 (34)	91.5268 (19)
γ (°)	90	90	90
V (Å)^3	2206.9 (6)	2218.8 (7)	2219.7 (5)

4.2. Temperature scaling

On exposure of a crystal to laser radiation the thermal parameters will increase compared to those of the light-OFF structure measured at the nominal temperature. As discussed above this is taken into account in the response ratio refinement by multiplying all the light-OFF thermal parameters by a temperature scaling parameter k_B. k_B can be estimated from the photo-Wilson plots using equation (7). For the example discussed here this gives a value of k_B = 1.70 when only the zinc, sulfur and chlorine U_{ij} are taken into account in the calculation of $\langle U_{\rm eq}\rangle$. This value indicates a significant temperature change in this experiment on exposure at a nominal temperature of 30 K. However, the increase of the k_B values above a value of one is not solely due to increased thermal vibration. The presence of static disorder in photo-excited crystals contributes to the estimate of k_B. Based on a model calculation on a photosensitive Cu(I) complex, Vorontsov & Coppens (2005) estimated the latter effect to be ∼20%. Multiplication of ΔB by 0.8 leads to a new estimate of k_B = 1.56.

An alternative way to estimate the temperature change is by examination of the ground-state unit-cell parameters at different temperatures, assuming the effect of structural changes on the cell dimensions to be secondary. In Table 1 the unit cell for the light-ON data is compared with that of a light-OFF data set measured at higher temperature (90 K) in a second experiment The unit-cell dimensions and volume are approximately equal for the 30 K light-ON and 90 K light-OFF data. The estimate of the temperature increase on exposure is supported by comparison of the photo-Wilson plots with temperature-Wilson plots, shown in Fig. 2. The plots are obtained by a scale-factor refinement of the high-temperature (90 K) data with the low-temperature (30 K) structural model and plotting the $I_{\rm obs}$(90 K)/$I_{\rm obs}$(30 K) ratios.

Table 2
Mean-square displacements, $\langle u^2\rangle_i$ (Å^2), along the principal ellipsoid axes at 30 and 90 K and corresponding eigenvector components (Å) from refinement of the data with $F_o^2 > 3\sigma(F_o^2)$.

The k_B' values in the last column are derived from the ratios of the ith pair of mean-square displacements $\langle u^2(90\text{ K})\rangle_i/\langle u^2(30\text{ K})\rangle_i$.

		T = 30 K				T = 90 K				
Atom	Parameter	$\langle u^2\rangle_i$	x_{ix}	x_{iy}	x_{iz}	$\langle u^2\rangle_i$	x_{ix}	x_{iy}	x_{iz}	k_B'
Zn1	$\langle u^2\rangle_1$	0.0112	0.145	0.914	−0.378	0.0193	0.136	0.888	−0.439	1.72
	$\langle u^2\rangle_2$	0.0101	0.070	0.375	0.924	0.0180	−0.085	0.456	0.886	1.78
	$\langle u^2\rangle_3$	0.0085	0.987	−0.160	0.020	0.0135	0.983	−0.082	0.163	1.59
Cl1	$\langle u^2\rangle_1$	0.0253	−0.063	0.971	0.232	0.0484	−0.089	0.981	0.170	1.91
	$\langle u^2\rangle_2$	0.0172	0.616	−0.142	0.775	0.0288	0.555	−0.093	0.827	1.67
	$\langle u^2\rangle_3$	0.0105	0.789	0.197	−0.581	0.0179	0.833	0.172	−0.527	1.70
Cl2	$\langle u^2\rangle_1$	0.0259	−0.544	0.569	0.617	0.0487	−0.524	0.593	0.612	1.88
	$\langle u^2\rangle_2$	0.0147	0.453	0.824	−0.339	0.0272	0.370	0.813	−0.450	1.85
	$\langle u^2\rangle_3$	0.0105	0.702	−0.092	0.706	0.0184	0.761	−0.009	0.648	1.75
S1	$\langle u^2\rangle_1$	0.0143	−0.226	0.649	0.726	0.0250	−0.302	0.580	0.757	1.75
	$\langle u^2\rangle_2$	0.0107	0.166	0.765	−0.622	0.0191	0.340	0.813	−0.473	1.79
	$\langle u^2\rangle_3$	0.0096	0.952	0.019	0.304	0.0157	0.883	−0.112	0.456	1.64
S2	$\langle u^2\rangle_1$	0.0165	0.095	0.981	0.167	0.0281	0.057	0.968	0.246	1.70
	$\langle u^2\rangle_2$	0.0115	0.101	−0.173	0.980	0.0202	0.311	−0.248	0.917	1.76
	$\langle u^2\rangle_3$	0.0099	0.993	−0.076	−0.086	0.0160	0.955	0.024	−0.294	1.62

The temperature-Wilson plot gives a k_B value of 1.56, taking into account only the zinc, sulfur and chlorine U_{ij} values. This value matches quite well the value obtained from the photo-Wilson plots shown in Fig. 1, indicating that the estimate of an average temperature of 90 K in the laser-exposed crystal is reasonable.

4.3. The adequacy of the k_B formalism

As discussed above, the k_B formalism implicitly assumes that all U_{ij} values increase by the same factor and that the eigenvectors of the thermal vibration tensors which express the directions of the principal axes of the ellipsoids are not affected. The nature of the ellipsoids is illustrated in Fig. 3. To investigate the validity of this assumption, the eigenvalues and eigenvectors of the U_{ij} tensors of the Zn, Cl and S atoms of the 30 K dark and the 90 K dark data are compared in Table 2.

The k_B' value averaged over all atoms in Table 2 equals 1.74 with a mean deviation of 0.07, or 4.1%. There is also a small change in the principal axes' directions (∼8° on average), indicating the approximate nature of the k_B formalism. However, its application in photocrystallographic experiments seems justified, especially if the temperature changes are moderate, as is the case in single-pulse diffraction experiments performed at synchrotron sources. We note that the value of k_B from the average over the atomic displacement parameters (ADPs) of the heavier atoms of 1.74 (7) is larger than the value from the Wilson plot of 1.56 by 2.5 standard deviations of the former value.

5. Conclusions

The temperature increase in multi-pulse pump–probe experiments can be estimated from unit-cell changes, analysis of photo-Wilson plots and their comparison with temperature-Wilson plots, and by refinement of a temperature scaling factor. All three methods agree to within ∼10%, even in the case presented in which the temperature change from the initial 30 K temperature is as large as 60 K. The corrections

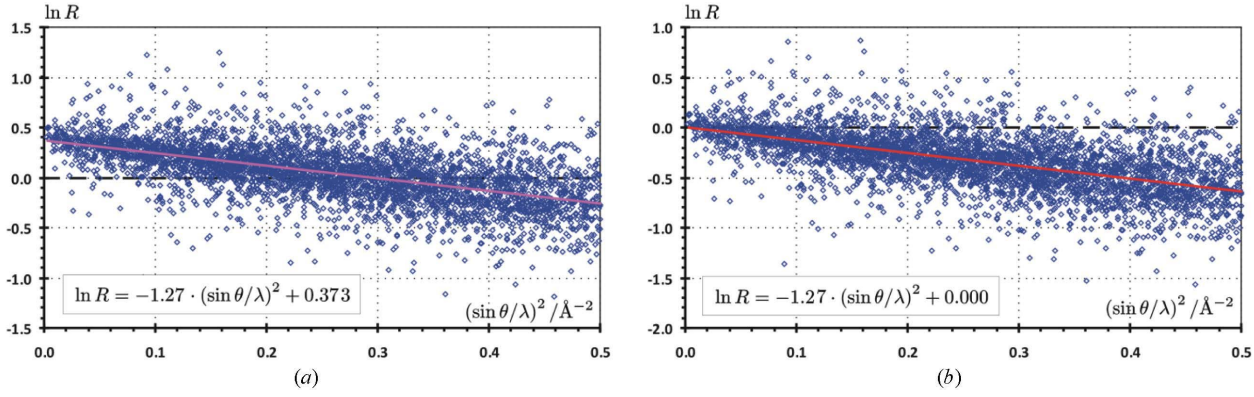

Figure 2
Temperature-Wilson plots comparing 30 K light-OFF and 90 K light-OFF data sets of (*a*) 90 K intensities brought on the absolute scale by scale-factor refinement using the 30 K structural model and (*b*) data from (*a*) corrected for the error in scaling of the 90 K data. In all cases only reflections with $I > 3\sigma(I)$ were included.

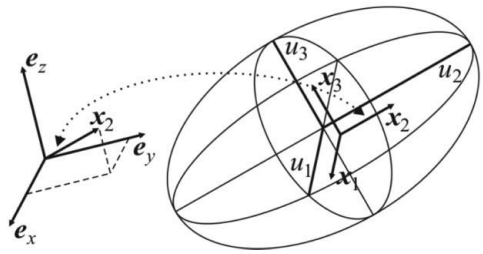

Figure 3
Schematic representation of thermal ellipsoid parameters used in Table 2. u_i – root-mean-square displacements along the principal axes, x_i – unit vectors along the principal directions ($\boldsymbol{e}_x$, $\boldsymbol{e}_y$, $\boldsymbol{e}_z$).

are much smaller when one or only a few laser pulses are applied prior to the interrogating X-ray pulse. Nevertheless, the methods discussed above should be applied in those cases also.

This research has been supported by the US National Science Foundation (grant No. CHE0843922). MSS is grateful to the Danish National Research Foundation and the Danish Strategic Research Council for financial support. RK would like to thank the Foundation for Polish Science for financial support within the 'International PhD Projects' program.

References

Blessing, R. H. (1995). *Acta Cryst.* A**51**, 33–38.
Blessing, R. H. (1997). *J. Appl. Cryst.* **30**, 421–426.
Bruker (2007). *SAINT*. Bruker AXS Inc., Madison, Wisconsin, USA.
Cailleau, H., Lorenc, M., Guérin, L., Servol, M., Collet, E. & Buron-Le Cointe, M. (2010). *Acta Cryst.* A**66**, 189–197.
Collet, E. (2010). Editor. *Dynamical Structural Science*, Special Issue, *Acta Cryst.* A**66**, Part 2, pp. 133–280.
Coppens, P., Kamiński, R. & Schmøkel, M. S. (2010). *Acta Cryst.* A**66**, 626–628.
Kim, C. D., Pillet, S., Wu, G., Fullagar, W. K. & Coppens, P. (2002). *Acta Cryst.* A**58**, 133–137.
Ozawa, Y., Pressprich, M. R. & Coppens, P. (1998). *J. Appl. Cryst.* **31**, 128–135.
Sheldrick, G. M. (2008). *Acta Cryst.* A**64**, 112–122.
Vorontsov, I. I. & Coppens, P. (2005). *J. Synchrotron Rad.* **12**, 488–493.
Vorontsov, I., Pillet, S., Kamiński, R., Schmøkel, M. S. & Coppens, P. (2010). *J. Appl. Cryst.* **43**, 1129–1130.
Woike, T. & Schaniel, D. (2008). Editors. *Photocrystallography*, Special Issue, *Z. Kristallogr.* **233**, Issues 4–5.